

Study on the Relationship Between Structure of Supramolecular Ion Material and Performance of Humidity Sensing

TANG Hui-min^{1,2}, YAN Hai-long², ZHANG Li², FEI Jun-jie^{1*}, YU Ping^{2*}, MAO Lan-qun²

1. *Key Laboratory of Environmental Friendly Chemistry and Applications of Ministry of Education, College of Chemistry, Xiangtan University, Xiangtan, Hunan 411105, China;*
2. *Beijing National Laboratory for Molecular Sciences, Key Laboratory of Analytical Chemistry for Living Biosystems, Institute of Chemistry, the Chinese Academy of Sciences, Beijing 100190*

Abstract: Humidity measurement and control is one of the most notable issues in various areas, such as climate, industry, agriculture, electronics, especially human comfort and health. In our previous study, we have found a new kind of supramolecular ionic material (SIM), consisting of an imidazolium-based dication (e.g., 1,10-bis(3-methylimidazolium-1-yl) decane, C₁₀(mim)₂) and electroactive dianionic (e.g., 2,2'-azino-bis(3-ethylbenzothiazoline-6-sulfonic acid), ABTS), shows ultrasensitive and ultrafast response towards humidity sensing. Herein we prepared six kinds of imidazolium-based dications with different carbon chain length (i.e., C₄, C₆, C₈, C₁₀, C₁₂, C₁₄), and found that three of them (i.e., C₁₀, C₁₂, C₁₄) could form water-stable SIM with ABTS. Cyclic voltammetry, chronoamperometry and quartz crystal microbalance were used to characterize the humidity sensing performance of these supramolecular ionic materials. The results show that

C₁₂-based SIM has the best humidity sensing performance compared with the other two kinds of SIM. Moreover, SEM images shows that the thickness of the ionic material became thinner with the increase of the carbon chain. We thus conclude that both the hydrophobic interaction and the specific surface area of SIMs would contribute to the performance of humidity response. This paper would lay the foundation for the development of new ionic compound for humidity sensing.

CLC Number: O646

Document Code: A

Introduction

Relative humidity (abbreviated as *RH*), defined as the ratio of the partial pressure of water vapor to the equilibrium vapor pressure of water at the same temperature, is considered as a key parameter in many fields^[1], such as climate, industry, agriculture, electronics, especially human comfort and health^[2-4]. Importantly, the rate at which perspiration evaporates on the human skin would be modulated under various humid conditions because human body uses evaporative cooling as the primary mechanism to regulate temperature. Hence, environmental humidity is always closely related to our life, and humidity measurement and control is one of the most notable issues in various areas. Additionally, given the obvious characteristics of high moisture in expiratory air of human and small tidal volume and high respiratory rate of adult rats, it is greatly inspiring for us to develop a high-performance humidity sensor with ultrasensitive and ultrafast humidity response, and realize the real-time recording for different respiratory patterns indirectly. To this end, the reliable and specific detection of humidity with excellent temporal resolution is quite essential. Up to now, different transduction techniques have been explored in order to improve sensitivity^[5-9], responsibility and recovery time, by exploiting different properties as read-out signal^[10-13], including electrical (current, impedance, capacitance) and optical characteristics as well as surface acoustic wave and quartz crystal microbalance. The reported sensing materials^[14] mainly include inorganic materials in the

form of nanowires, nanoflakes, nanotubes of metal oxides, ceramics, and perovskites, and other numerous components comprising of polyelectrolyte, carbon based derivatives and ionic liquids also have been employed as active elements.

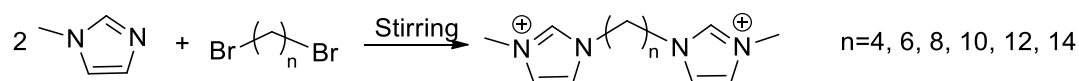
Electrical humidity-sensing electrodes allow for real-time detection of humidity with high sensitivity and selectivity. Among of the material for electrical humidity-sensing, ion compounds are particular attractive due to its strong interaction with water^[15-20]. However, traditional ionic salts (e.g., calcium chloride, magnesium chloride, and zinc chloride) was difficult used to fabricated humidity sensing due to its easily deliquescent^[21]. We have prepared a new kind of supramolecular ionic material (SIM) composed of an imidazolium-based dication (e.g., 1,10-bis(3-methylimidazolium-1-yl) decane, C₁₀(mim)₂) and electroactive dianionic (e.g., 2,2'-azino-bis(3-ethylbenzothiazoline-6-sulfonic acid), ABTS), which bears sensitive and fast response towards humidity sensing^[22]. More importantly, the low driving potential (i.e., 0.5 V) was used compared with other kinds of humidity sensing material^[23] (e.g., nafion, 5 V). These excellent properties enable the SIM-based humidity sensors for monitoring the respiratory rate of both humans and living rats.

Herein, we prepared six kinds of imidazolium-based dications with different carbon chain length (C₄, C₆, C₈, C₁₀, C₁₂, C₁₄) as shown in **Figure 1A**, and found that three of them (i.e., C₁₀, C₁₂, C₁₄) could form water-stable SIM with ABTS as shown in **Figure 1B**. We have systematically studied the relationship between the structure of SIM and the performance of humidity response, and found that the SIM with C₁₂ bears the most sensitive response toward humidity. Morphology results indicating that both the hydrophobic interaction and the specific surface area of SIMs would contribute to the performance of humidity response. This paper would provide a reference for the development of new ionic compound towards humidity sensing.

Experimental Section

Chemicals. 2,2'-hydrazine-bis(3-ethyl-benzothiazole-6-sulfonic acid) diammonium salt (ABTS), 1-methylimidazole, 1,4-dibromobutane, 1,6-dibromohexane, 1,8-dibromooctane, 1,10-dibromodecane, 1,12-Dibromododecane, 1,14-dibromotetradecane all obtained from Sigma-Aldrich and used as supplied. LiCl, CH₃COOK, MgCl₂, K₂CO₃, Mg(NO₃)₂, CuCl₂, NaCl, KCl and K₂SO₄ all obtained from Aladdin Reagent Co. (China) and used without further purification. Au interdigital electrode (IDE) was purchased from Jihua Co., Siping, China, which was 300- μ m electrode width and 100- μ m electrode separation, and twelve pairs of electrodes were printed onto a ceramic substrate (15 mm \times 10 mm \times 1 mm). Prior to the modification, the IDE was cleaned in piranha solution followed by washing in distilled water several times and then dried by nitrogen flow. All aqueous solutions were prepared with Milli-Q water.

Synthesis of Dications. The dications were synthesized with the procedures reported previously^[24].



Typically, 1,4-dibromobutane, 1,6-dibromohexane, 1,8-dibromooctane, 1,10-dibromodecane, 1,12-dibromododecane or 1,14-dibromotetradecane (50 mmol) was added to 1-methylimidazole (100 mmol) in a round bottom flask under constant stirring at room temperature for 2 hours. The bromide salt was dissolved in 50 mL water and extracted with ethyl acetate for 3 times. Water was removed using rotary evaporator, and the resulting salts were dried in vacuum drying oven. The structures of C_n(mim)₂ (n=4, 6, 8, 10, 12, 14) were confirmed by ¹H-NMR, the peak assignments of ¹H-NMR spectra were as follows.

C₄(mim)₂: ¹H-NMR (DMSO, 400MHz): δ ppm 9.32(s, 2H); 7.84(s, 2H); 7.75(s, 2H), 4.26(t, 4H); 3.87(s, 6H); 1.79(s, 4H).

C₆(mim)₂: 1H-NMR (DMSO,400MHz): δ ppm 9.32(s, 2H); 7.86(t, 2H); 7.76(t, 2H), 4.20(t, 4H); 3.88(s, 6H); 1.80(t, 4H); 1.29(t, 4H).

C₈(mim)₂: 1H-NMR (DMSO,400MHz): δ ppm 9.27(s, 2H); 7.83(s, 2H); 7.75(s, 2H), 4.17(t, 4H); 3.86(s, 6H); 1.77(t, 4H); 1.26(s, 8H).

C₁₀(mim)₂: 1H-NMR (DMSO,400MHz): δ ppm 9.24(s, 2H); 7.81(t, 2H); 7.74(t, 2H), 4.17(t, 4H); 3.86(s, 6H); 1.77(t, 4H); 1.26(s, 12H).

C₁₂(mim)₂: 1H-NMR (DMSO,400MHz): δ ppm 9.34(s, 2H); 7.86(t, 2H); 7.78(t, 2H), 4.18(t, 4H); 3.87(s, 6H); 1.76(t, 4H); 1.21(s, 16H).

C₁₄(mim)₂: 1H-NMR (DMSO,400MHz): δ ppm 9.34(s, 2H); 7.84(t, 2H); 7.64(t, 2H), 4.20(t, 4H); 3.93(s, 6H); 1.78(t, 4H); 1.27(s, 20H).

Apparatus. The morphology and size of the materials were characterized by field emission scanning electron microscopy (FE-SEM, Hitachi SU-8020) at an accelerating voltage of 10 kV. Humidity sensing experiments were performed by using a CH Instruments model 660E electrochemical analyzer (Shanghai, China). Quartz crystal microbalance experiment is completed by a CH Instruments model 440 electrochemical analyzer (Shanghai, China) and a syringe pump (Harvard Apparatus PHD 2000).

Humidity Response. Firstly, 1mg of the C_n-based SIM (e.g., C₁₀-based SIM) was dispersed in 1 mL of deionized water to form a homogeneous dispersion. Then, 300 μ L of the as-prepared solution was dipped onto the surface of the gold interdigital electrode, first dried in air and then annealed at 60 °C for 4 h under vacuum, cooled in air. The conductive silver glue is used to connect the copper wire and the pads of the interdigitated electrode. The prepared electrode is then fixed in a special home-made setup^[22] with double-sided adhesive tape. The humidity was controlled using different solutions saturated with LiCl, CH₃COOK, MgCl₂, K₂CO₃, Mg(NO₃)₂, CuCl₂, NaCl, KCl, KNO₃, and K₂SO₄, and was simultaneously monitored by a commercial hygrometer (DT-615, Shenzhen, China). When the cyclic voltammetry was conducted, let the electrode stand in the device

for 10 minutes before starting the experiment, while for i-t experiment, every 50 seconds alternately switch moisture and nitrogen at the bias potential of 0.4 V.

Quartz Crystal Microbalance Experiment. In a 50 mL syringe, 20 mL of deionized water was placed in and kept the syringe horizontal until the *RH* above the water surface reached 100%. The water vapor was injected into the quartz crystal microbalance chamber at a rate of $0.2 \text{ mL}\cdot\text{min}^{-1}$ with a micro-syringe pump to keep the *RH* in the chamber at 100%. At the same time, a quartz wafer which was modified by $20 \mu\text{L}$ of $1 \text{ mg}\cdot\text{mL}^{-1}$ of SIM was placed in the chamber and its frequency change with time was recorded.

Results and Discussion

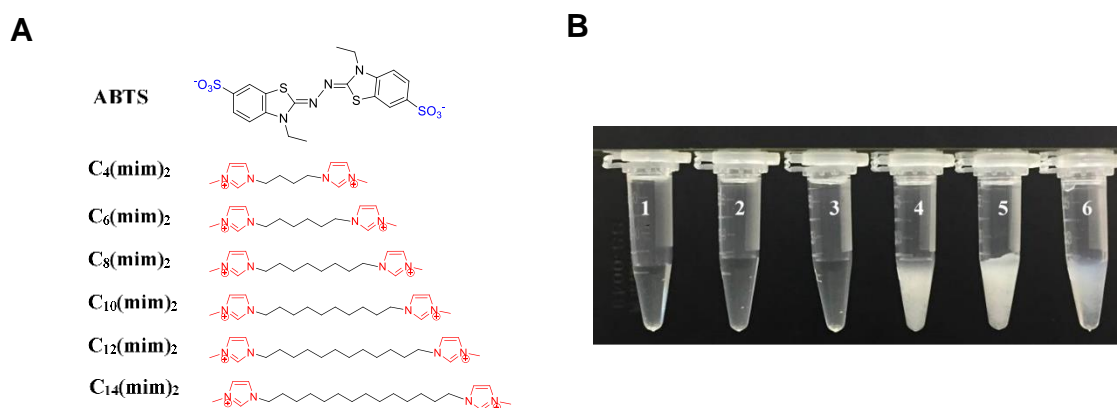


Figure 1. A) Chemical structures of ions investigated herein. B) Photograph of aqueous solution containing 10 mM ABTS mixed with equal amount of 10 mM dication solution (from vial 1 to vial 6: $\text{C}_4(\text{mim})_2$ to $\text{C}_{14}(\text{mim})_2$) and then centrifuged.

Before investigate the relationship between structure and humidity response, various kinds of imidazolium-based dications with different alkyl chain length were synthesized (structures shown in Figure 1A). Interestingly, we found that, when the same concentration (10 mM) of aqueous solutions of bromide salts of dications (1-6) were mixed into the aqueous solutions of the amino salt of ABTS

dianion (10 mM), different phenomena were observed, as typically shown in Figure 1B. Similar to that obtained with C_{10} , the mixing of the aqueous solution of C_{12} and C_{14} with that of ABTS quickly forms white aggregates, while the mixing of those of other dications with shorter alkyl chain length (i.e., C_4 , C_6 and C_8) with that of ABTS do not form any aggregates, even the mixtures were centrifuged. This result demonstrates that, although all ionic complexes bear the same groups of cations and anions, they may have different associate constant due to the different substituted groups just like the inorganic salt NaCl and AgCl. This could be understood from two different ways. One is the hydrophobic property of alkyl chain. When the alkyl chain length increases, the hydrophobicity of the dications increases and thereby the water solubility of the as-formed complex decreases. The other possible reason was the increase in the alkyl chain length, which could influence the charge density of the imidazolium. Moreover, the charged species with two charges is favorable to form supramolecular ionic network and thus keep the high water stability. The formed insoluble supramolecular ionic materials were named as C_{10} -ABTS, C_{12} -ABTS and C_{14} -ABTS, respectively.

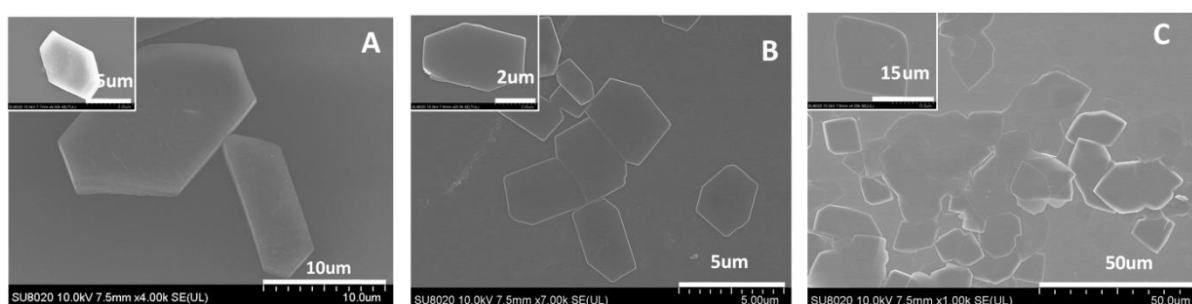


Figure 2. SEM images of the as-prepared supramolecular material: A) C_{10} -ABTS, B) C_{12} -ABTS; C) C_{14} -ABTS.

The nanostructures of the as-prepared SIMs were characterized by SEM. As shown in Figure 2, the hexagonal microstructure was formed for C_{10} -ABTS, the size of the hexagonal structure ranges

from several to tens of micrometers with the thickness varying from hundreds of nanometers to several micrometers. With the increase of the carbon chain, the morphology was changed from hexagonal microstructure to quadrangle structure. Moreover, the thickness was decreased with the increase of carbon chain. For C₁₄-ABTS, very thin film was obtained with the thickness of several nanometers.

We then studied the humidity response of the as-prepared SIMs. As shown in Figure 3A, at the specific relatively humidity, the C₁₂-ABTS (black curve) shows the largest conductivity compared with that of C₁₀-ABTS (blue curve) and C₁₄-ABTS (red curve). We also conducted the humidity response by using chronoamperometry. As shown in Figure 3B, all three kinds of SIMs show the obvious response towards humidity when the humidity changed from nitrogen atmosphere to 54% relatively humidity. Similar with the result from the cyclic voltammetry, C₁₂-ABTS (black curve) shows the largest current response compared with that of C₁₀-ABTS (blue curve) and C₁₄-ABTS (red curve) as shown in Figure 3B.

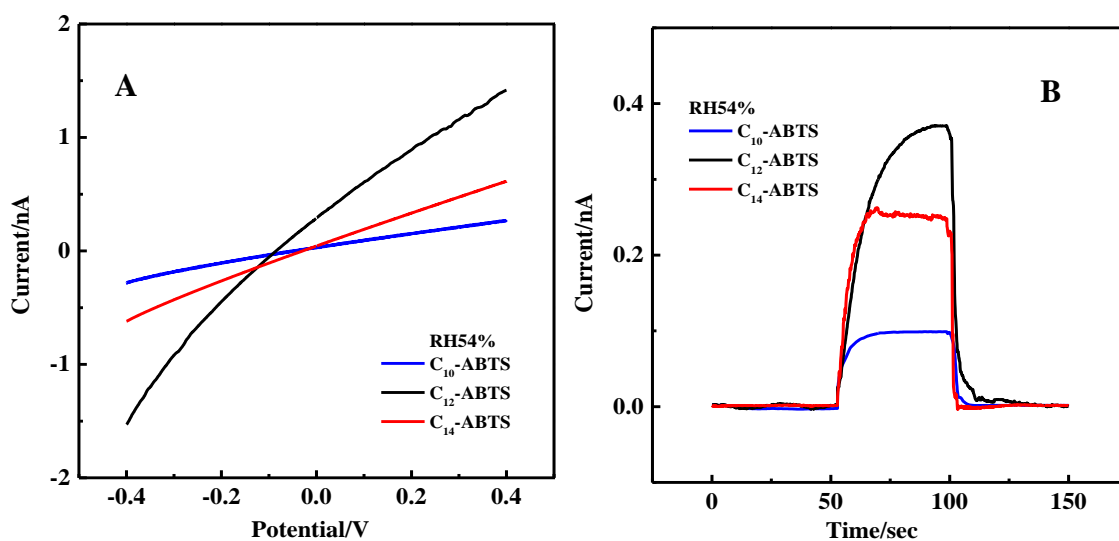


Figure 3. A) $I-V$ curves of the C_n-based SIM (n=10,12,14) under RH 54% atmospheres at room temperature. B) The typical amperometric response of C_n-ABTS (n=10,12,14) to RH 54% condition.

To understand the origin of the largest humidity response of C₁₂-ABTS, quartz crystal microbalance (QCM) was used to investigate hygroscopicity of the as-prepared SIMs as shown in Figure 4. In contrast to bare Au plate with negligible frequency shift at RH 100%, all the SIMs with different carbon chain-coated Au plates show noticeable frequency change. Moreover, the largest frequency change was obtained for the C₁₂-ABTS film, essentially suggesting a stronger hygroscopicity of C₁₂-ABTS than that of C₁₀-ABTS and C₁₄-ABTS. Compared with C₁₀-ABTS, C₁₂-ABTS bears a larger specific area due to the decrease of the thickness. While C₁₄-ABTS has the more hydrophobic carbon chain compared with C₁₂-ABTS, which would limit its hydrogroscopicity. Therefore, we think that the balance of specific area and the hydrophobicity of the SIM plays a key role for the high sensitive high humidity, which would provide a reference for the design of new ionic compounds for humidity sensing.

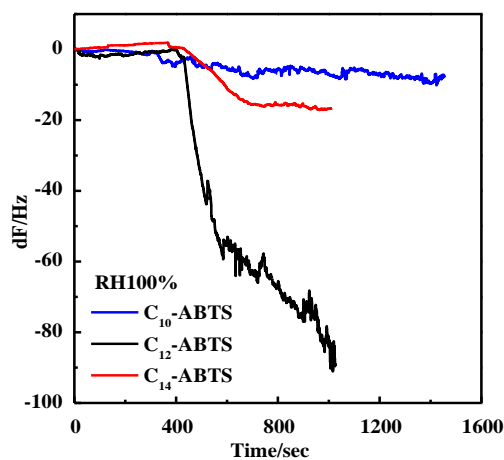


Figure 4. The frequency response of C_n-based SIM (n=10,12,14) quartz crystal microbalance to RH 100% condition.

Conclusion

In summary, we have investigated the relationship between the structure of C_n-based SIM (also named as C_n-ABTS, n=10,12,14) and the performance of humidity response with three kinds of

techniques (i.e., I-V curve, chronoamperometry and quartz crystal microbalance). SEM images show that the thickness of the ionic material became thinner with the increase of the carbon chain. The increase of carbon chain enhances the hydrophobic interaction and further increases the specific surface area of the ionic material as well. These two effects have opposite impacts on the moisture sensing ability of these ionic materials, and the results show that the humidity sensing performance of C₁₂-ABTS is the best. Therefore, we think that both the hydrophobic interaction and the specific surface area of SIMs would contribute to the performance of humidity response. This paper would lay the groundwork for the development of new ionic compound for humidity sensing.

References

- [1] Delapierre G, Grange H, Chambaz B, et al. Polymer-based capacitive humidity sensor: characteristics and experimental results[J]. *Sensors and Actuators B: Chemical*, 1983, 4(1):97-104.
- [2] Xu H F(徐洪峰), Liu J(刘晶), Wan L(万莉). Perfluorinated Sulfonic Acid Lithium Conductivity Humidity Sensor[J]. *Journal of Electrochemistry(电化学)* 2003,9(02):217-221.
- [3] Edmonds Z V, Mower W R, Lovato L M, et al. The reliability of vital sign measurements[J]. *Annals of Emergency Medicine*, 2002, 39(3):233-237.
- [4] Ghosh J J, Quastel J H. Narcotics and brain respiration[J]. *Nature*, 1954, 174(4418):28-31.
- [5] Kulwicki B M. Humidity Sensors[J]. *Journal of the American Ceramic Society*, 2010, 74(4):697-708.
- [6] Ogura K, Fujii A, Shiigi H, et al. Effect of hygroscopicity of insulating unit of polymer composites on their response to relative humidity[J]. *Journal of the Electrochemical Society*, 2000, 147(3):1105–1109.
- [7] Christie J H, Krenk S H, Woodhead I M. The electrical properties of hygroscopic solids[J]. *Biosystems Engineering*, 2009, 102(2):143-152.

- [8] Tobjörk D, Österbacka R. Paper electronics.[J]. *Advanced Materials*, 2011, 23(17):1935-1961.
- [9] Karimov K S, Fatima N, Sulaiman K, et al. Sensitivity enhancement of OD-and OD-CNT-based humidity sensors by high gravity thin film deposition technique[J]. *Journal of Semiconductors*, 2015, 36(3):69-73.
- [10] Wang G, Wang Q, Lu W, et al. Photoelectrochemical study on charge transfer properties of TiO₂-B nanowires with an application as humidity sensors[J]. *Journal of Physical Chemistry B*, 2006, 110(43):22029-22034.
- [11] Chang S P, Chang S J, Lu C Y, et al. A ZnO nanowire-based humidity sensor[J]. *Superlattices and Microstructures*, 2010, 47(6):772-778.
- [12] Zhang Y, Yu K, Ouyang S, et al. Detection of humidity based on quartz crystal microbalance coated with ZnO nanostructure films[J]. *Physica B: Condensed Matter*, 2005, 368(1):94-99.
- [13] Xu J, Zhang W X, Yang Z H, et al. Large-Scale Synthesis of Long Crystalline Cu_{2-x}Se Nanowire Bundles by Water-Evaporation-Induced Self-Assembly and Their Application in Gas Sensing[J]. *Advanced Functional Materials*, 2010, 19(11):1759-1766.
- [14] Chen Z, Lu C. Humidity Sensors: A Review of Materials and Mechanisms[J]. *Sensor Letters*, 2005, 3(4):274-295.
- [15] Schneider H. Linear free energy relationships and pairwise interactions in supramolecular chemistry[J]. *Chemical Society Reviews*, 1994, 23(4):227-234.
- [16] Gunawan C A, Ge M, Zhao C. Robust and versatile ionic liquid microarrays achieved by microcontact printing[J]. *Nature Communications*, 2014, 5(4):3744-3742.
- [17] Decher G. Fuzzy Nanoassemblies: Toward Layered Polymeric Multicomposites[J]. *Science*, 1997, 277(5330):1232-1237.
- [18] Faul C F J, Antonietti M. Ionic Self-Assembly: Facile Synthesis of Supramolecular Materials [J]. *Advanced Materials*, 2010, 15(9):673-683.

- [19] Zakrevskyy Y, Faul C, Guan Y, et al. Alignment of a Perylene-Based Ionic Self-Assembly Complex in Thermotropic and Lyotropic Liquid-Crystalline Phases[J]. *Advanced Functional Materials*, 2010, 14(9):835-841.
- [20] Buzzeo M C, Hardacre C, Compton R G. Use of Room Temperature Ionic Liquids in Gas Sensor Design[J]. *Analytical Chemistry*, 2004, 76(15):4583-4588.
- [21] Dunmore, F W, An Electric Hygrometer and Its Application to Radio Meteorography [J]. *Journal of Research of the National Bureau of Standards*, 1938, 20(6): 723-744.
- [22] Yan H, Zhang L, Yu P, et al. Sensitive and Fast Humidity Sensor Based on A Redox Conducting Supramolecular Ionic Material for Respiration Monitoring[J]. *Analytical Chemistry*, 2017, 89(1):996-1001.
- [23] Kuban P, Berg J M, Dasgupta P K. Durable microfabricated high-speed humidity sensors[J]. *Analytical Chemistry*, 2004, 76(9):2561-2567.
- [24] Anderson J L, Ding R, Arkady E A, et al. Structure and Properties of High Stability Geminal Dicationic Ionic Liquids[J]. *Journal of the American Chemical Society*, 2005, 127(2):593-604.

基于超分子离子晶体的湿度传感构效关系研究

唐会敏^{1,2}, 颜海龙², 张丽², 费俊杰^{1*}, 于萍^{2*}, 毛兰群²

(1. 湘潭大学化学学院环境友好化学与应用教育部重点实验室, 中国湖南湘潭 411105; 2. 北京分子科学国家实验室, 中国科学院化学研究所活体分析化学重点实验室, 中国北京 100190)

摘要: 相对湿度是许多领域的关键参数, 环境湿度与我们的生活密切相关, 因此对湿度进行测量和控制是各个领域值得关注的问题之一. 在我们前期的研究中, 我们制备了一种新型的超分子离子材料 (SIM), 它是由基于咪唑的双阳离子 (如, 1,10-双 (3-甲基咪唑-1-基) 癸烷, C₁₀(mim)₂) 和电活性二阴离子 (例如, 2,2'-连氨基-双 (3-乙基苯并噻唑啉-6-磺酸), ABTS) 组成的, 发现其对湿度具有敏感且快速的响应. 在此基础上, 本文制备了 6

种不同碳链 (C₄, C₆, C₈, C₁₀, C₁₂, C₁₄) 的咪唑基化合物, 发现其中 3 种 (C₁₀, C₁₂, C₁₄) 可与 ABTS 形成水稳定的 SIM. 循环伏安法, 计时电流法以及石英晶体微量天平表征了这些超分子离子材料的湿度传感性能, 发现基于 C₁₂ 的 SIM 具有最佳的湿度传感性能. 同时, SEM 结果显示随着碳链的增加, 离子材料的厚度变薄并且形态变得不规则. 因此, 我们认为疏水作用和材料比表面积均会影响湿度传感的灵敏度. 本研究为发展新的湿度响应的离子传感材料奠定了基础.